Scaling effects of relaxor-$PbTiO_3$ crystals and composites for high frequency ultrasound

Hyeong Jae Lee, Shujun Zhang,[a] and Thomas R. Shrout
Department of Materials Science and Engineering, Materials Research Institute, The Pennsylvania State University, University Park, Pennsylvania 16802, USA

(Received 15 January 2010; accepted 2 May 2010; published online 24 June 2010)

The dielectric and piezoelectric properties of $Pb(Mg_{1/3}Nb_{2/3})O_3-PbTiO_3$ (PMN-PT) and $Pb(In_{1/2}Nb_{1/2})O_3-Pb(Mg_{1/3}Nb_{2/3})O_3-PbTiO_3$ (PIN-PMN-PT) ferroelectric single crystals were investigated as a function of thickness/scale in monolithic and piezoelectric/polymer 1–3 composites. For the case of PMN-PT single crystals, the dielectric ($\varepsilon_{33}^T/\varepsilon_0$) and electromechanical properties (k_{33}) were found to significantly decrease with decreasing thickness (500–40 μm), while minimal thickness dependency was observed for PIN-PMN-PT single crystals. Temperature dependent dielectric behavior of the crystals suggested that the observed thickness dependence in PMN-PT was strongly related to their relatively large domain size (>10–20 μm). As anticipated, 1–3 composite comprised of PIN-PMN-PT crystals exhibited superior properties to that of PMN-PT composite at high frequencies (>20 MHz). However, the observed couplings, being on the order of 80%, were disappointedly low when compared to their monolithic counterparts, the result of surface damage introduced during the dicing process, as evidenced by the broadened [002] peaks in the x-ray diffraction pattern. © *2010 American Institute of Physics*. [doi:10.1063/1.3437068]

I. INTRODUCTION

Ultrasound imaging is a well-established medical imaging modality that provides noninvasive diagnostic information of living tissue and organs. Traditionally, ultrasonic imaging is used in the area of cardiology, obstetrics, and abdominal diagnosis.[1,2] In these applications, the ultrasound frequency is below 10 MHz allowing deeper penetration at the expense of resolution. Recently, there is growing need for higher resolution, particularly in the areas of dermatology, ophthalmology, and intravascular imaging, leading to the research and development of high frequency ultrasound transducers (20–100 MHz).[3–5]

A piezoelectric material is an important component in ultrasound transducers. The thickness of the piezoelectric element defines the operational frequency of the transducer through the frequency constant ($N=f\times t$, where N is the frequency constant, f the frequency, and t the thickness). High dielectric ($\varepsilon_{33}^T/\varepsilon_0$) and electromechanical coupling (k_t) of piezoelectric materials are often desired for high frequency arrays and small aperture single element transducers, offering improved electrical matching to the imaging electronics and increased bandwidth and sensitivity.[6–8]

Among the wide range of piezoelectric materials, relaxor-$PbTiO_3$ (PT) single crystals, such as $Pb(Mg_{1/3}Nb_{2/3})O_3-PbTiO_3$ (PMN-PT), have attracted interest for ultrasound transducers due to their excellent dielectric and electromechanical properties (e.g., $\varepsilon_r>6000$, $k_{33}>0.9$).[9] In particular, a newly developed ternary single crystal system, $Pb(In_{1/2}Nb_{1/2})O_3-Pb(Mg_{1/3}Nb_{2/3})O_3-PbTiO_3$ (PIN-PMN-PT) offers increased coercive fields (~5 kV/cm) and improved thermal stability (>120 °C) compared to binary PMN-PT crystals.[10,11] In contrast to polycrystalline ceramics, e.g., $Pb(Zr,Ti)O_3$, crystals do not suffer from grain size issues, potentially eliminating scaling limitations which may be associated with high frequency transducers.

To date, however, the thickness dependent properties of relaxor-PT single crystals have yet to be investigated. Recent experimental data for PMN-PT 1–3 crystal/epoxy composites operating at frequencies ≥40 MHz have reported a large decrease in electromechanical coupling, leading to the question of the origin of the degradation.[12,13]

In this work, the dielectric and electromechanical properties of PMN-PT and PIN-PMN-PT monolithic plate resonators and 1–3 composites were investigated as a function of scale/thickness and/or corresponding ultrasound frequency.

II. EXPERIMENTAL

Relaxor-PT single crystals, including PMN-PT and PIN-PMN-PT were obtained from TRS technologies Inc., which were grown using the modified Bridgman method.[14] Samples with various thicknesses were prepared by lapping and polishing. Initial lapping utilized 15 μm Al_2O_3 powder suspended in a distilled water medium. Final polishing was carried out with a 0.05 μm diamond paste to minimize surface damage. Vacuum sputtered gold was applied to the parallel surfaces of the samples as the electrodes. The samples were then drilled to the desired dimensions with diameter to thickness ratios of ≥20. The large aspect ratio ensured that lateral mode harmonics would not interfere with the fundamental thickness mode. All samples were annealed at 400 °C for 5 h in order to alleviate residual stress. Prior to electrical measurements, PMN-PT and PIN-PMN-PT single crystals were poled for 3 min at room temperature under fields of 10 kV/cm and 20 kV/cm, respectively.

[a]Author to whom correspondence should be addressed. Electronic mail: soz1@psu.edu.

For the fabrication of 1–3 piezocrystal/epoxy composites, the samples were diced using an automatic dicing machine, K&S 982–6 (Kulicke & Soffa Industries, Willow Grove, PA) with different sizes of blades depending on the frequency of interest. For transducers operating below 10 MHz, 1–3 composites were machined with a 50×762 μm^2 nickel bond dicing blade (Dicing Blade Technology, Inc.), and a 26×586 μm^2 nickel bond dicing blade (Asahi Diamond, Inc.). For transducers operating above 10 MHz, the samples were diced using 2–4 μm grit, 12×343 μm^2 nickel bonded diamond blade (Asahi Diamond, Inc.). The samples were first diced along one direction with a spindle speed of 30 000 rpm and a feed rate of 1.5 mm/sec. The samples were then diced in the perpendicular direction using the same dicing conditions. A low viscosity epoxy (Epotek 301, Bellerica, MA) was then backfilled into the kerfs in vacuum for 30 min, and subsequently cured at room temperature for 24 h. The fabricated composites were polished until all the piezoelectric posts were exposed, and gold electrodes were sputtered on both surfaces. The PMN-PT and PIN-PMN-PT composites were then poled at room temperature using fields of 10 kV/cm and 20 kV/cm for 3 min, respectively.

The dielectric properties of the various samples were characterized using an HP4294A impedance-phase gain analyzer. The free ($\varepsilon_{33}^T/\varepsilon_0$) and clamped ($\varepsilon_{33}^S/\varepsilon_0$) permittivities were calculated from the capacitance values measured at a frequency of 1 kHz and twice the thickness antiresonance frequency, respectively. The dielectric behavior as a function of temperature was determined using a multifrequency HP4284A LCR meter connected to a computer-controlled furnace. The resonance and antiresonance frequencies of 1–3 composites were measured using an HP4294A impedance-phase gain analyzer. The electromechanical coupling factors were calculated from the measured resonance and antiresonance frequencies according to the IEEE standard.[15] Scanning electron microscopy (SEM, S-3500N, Hitachi, Tokyo, Japan) was used for examination of the edge surfaces of the composite posts. X-ray diffraction (XRD, PANalytical) was employed to determine the level of dicing damage on the piezoelectric elements, as reflected by peak broadening.

III. RESULTS AND DISCUSSION

The free ($\varepsilon_{33}^T/\varepsilon_0$) and clamped ($\varepsilon_{33}^S/\varepsilon_0$) dielectric permittivities of samples, with thicknesses ranging from 500–30 μm, are plotted in Fig. 1. Each value is the average of 3–5 samples, and the error bars represent the standard deviation. Thickness frequency constants for both PMN-PT and PIN-PMN-PT crystals were found to be ~2000 Hz m, maintaining the same values with varying thickness. The corresponding thickness resonance frequencies of the crystals were added on the top X-axis of Fig. 1.

From Fig. 1, it was found that the clamped permittivities of both PMN-PT and PIN-PMN-PT single crystals exhibited similar values across the range of thicknesses; however, the free permittivity of PMN-PT crystals was strongly affected by the sample scale. At a thickness of ~40 μm (corresponding frequency ~50 MHz), the free permittivity of PMN-PT crystals was reduced by half. In contrast, PIN-PMN-PT crystals exhibited minimal thickness dependent dielectric properties, even down to thicknesses ≤40 μm.

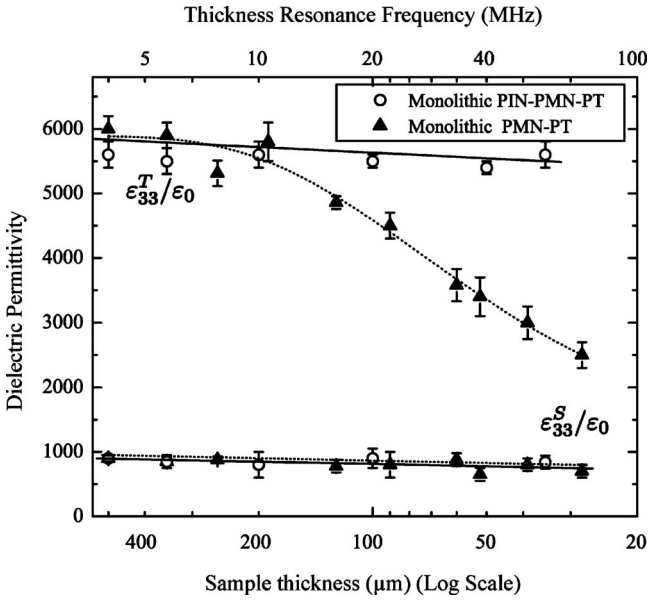

FIG. 1. Free and clamped dielectric permittivities of relaxor-PT crystals as a function of sample thickness and corresponding ultrasound frequency.

Property degradation in ferroelectric materials has been reported to be attributed to surface damage during sample preparation, resulting in the low polarizable layers/nonferroelectric layers.[16,17] A series capacitance model, in which damage layers exist in series with the normal ferroelectric portion, has been used to explain the degraded dielectric permittivity as function of the thickness of the nonferroelectric layers/samples.[18]

Property degradation in ferroelectric materials may also be associated with their respective domain sizes. It is well known that the dielectric and piezoelectric response of [001]-poled relaxor-PT single crystals is related to the engineered domain configuration and polarization rotation mechanism.[6,19,20] For [001] poled rhombohedral crystals, a stable multidomain structure "4R" is formed since only four of the eight possible polarization orientations, i.e., [111], $[\bar{1}11]$, $[1\bar{1}1]$, and $[\bar{1}\bar{1}1]$, remain in the crystals upon poling. For relatively thick samples (thickness ≫ domain sizes), the polarization can freely rotated from [111] to [001] directions under an external electric field, contributing to the dielectric and piezoelectric properties. However, when the physical thickness of the samples becomes on the order of the domain size, the boundary conditions may disrupt the equilibrium "4R" domain structures and restrict polarization rotation, resulting in property degradation.

To delineate the degradation mechanism(s) observed in this work, the dielectric properties were investigated as a function of temperature and thickness for relaxor-PT crystals. Figure 2 shows the temperature dependence of dielectric permittivity for PMN-PT samples with different thicknesses. For comparison, the dielectric behavior of PIN-PMN-PT crystals is given in the small inset. As observed, in the temperature range of 30 °C–T_{RT} (the rhombohedral to tetrago-

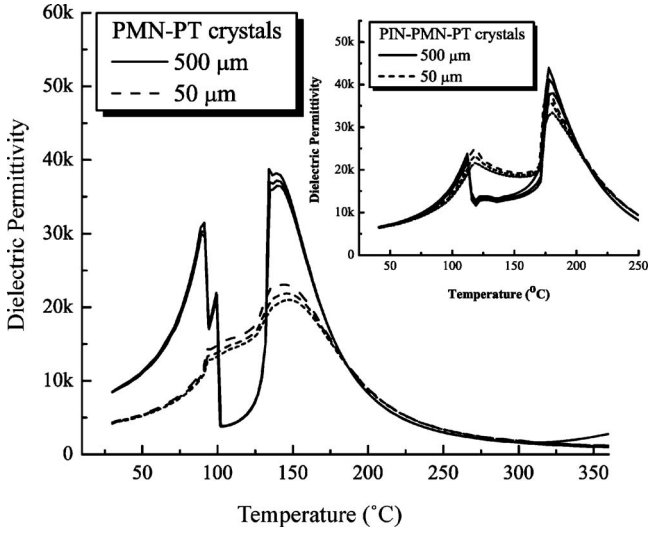

FIG. 2. Dielectric permittivity as a function of temperature for PMN-PT and PIN-PMN-PT crystals with different thicknesses.

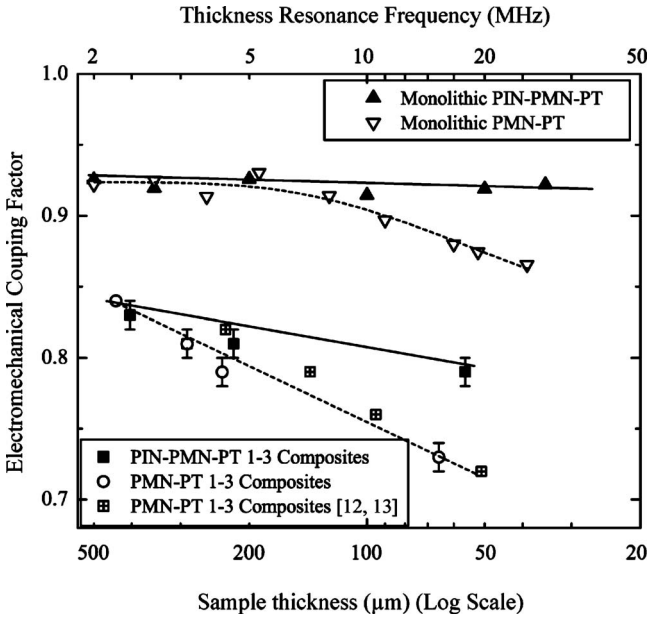

FIG. 3. Electromechanical coupling factor (k_{33}) for monolithic and crystal/epoxy 1–3 composites as a function of sample thickness and corresponding ultrasound frequency.

nal phase transition), PIN-PMN-PT crystals exhibited similar dielectric permittivities, regardless of the sample thickness. In contrast, the permittivity of thin PMN-PT samples was found to be significantly lower than the values of thick samples in the same temperature range. Of particular importance is that both PMN-PT and PIN-PMN-PT samples exhibited thickness independent dielectric behavior above the Curie temperature (T_C), where no ferroelectric domains exist. The above results indicate that the degraded dielectric properties observed in thin PMN-PT crystals could be attributed to the increased surface boundary effects due to their relatively large domain sizes. Preliminary domain observations revealed that poled PMN-PT single crystals were found to possess relatively large domain sizes ($\sim$10–20 μm) when compared to poled PIN-PMN-PT single crystals, whose domains were found to be on the order of $\sim$1 μm.

Figure 3 presents the electromechanical coupling factors (k_{33}) of 1–3 composites as a function of sample thickness and the corresponding resonance frequency. For comparison, the coupling (k_{33}) for monolithic and PMN-PT/epoxy 1–3 composites were included in Fig. 3.[12,13] The frequency constants (N_{33}) for both PMN-PT and PIN-PMN-PT 1–3 composites were found to be similar, on the order of $\sim$1000 Hz m. For the monolithic samples, the longitudinal coupling factors were calculated from the equation $[k_{33} = \sqrt{1-(\varepsilon_{33}^S/\varepsilon_{33}^T)}]$. As expected from the dielectric data (as shown in Fig. 1), the coupling of PIN-PMN-PT monolithic samples was found to maintain same values, being on the order of 93% over the entire frequency range (2–40 MHz). PMN-PT samples, however, exhibited decreased coupling for samples with frequencies above 10 MHz, related to the associated domain clamping and polarization rotation suppressing, when sample thickness reaching the size of domains (surface boundary effect).

From Fig. 3, PMN-PT/epoxy 1–3 composites were found to exhibit a noticeable decrease in coupling (k_{33}) with decreasing sample thickness, with coupling being on the order of 72% at 20 MHz, which is similar to that previously reported.[12,13] Of particular significance is that PIN-PMN-PT/epoxy 1–3 composites were found to maintain relatively high coupling factors, being on the order of $\geq$80% over the thickness range studied (500–50 μm). However, these values are far less than the expected values determined from monolithic samples, being on the order of >90%, indicating that 1–3 composites may contain surface damage layers/low polarizable layers caused by the dicing process.

Figure 4 shows an SEM image of a diced PMN-PT crystal composite without epoxy filling. The image shows no noticeable macroscopic damage, such as chipping and post-breakage. Similar images were also observed for diced PIN-PMN-PT crystal composites.

X-ray analysis of PMN-PT and PIN-PMN-PT single crystals are given in Fig. 5. It was found that the [002] XRD profiles of diced surfaces exhibited peak broadening, compared to those of polished surfaces. This confirms that mechanical dicing can produce highly stressed and/or damaged

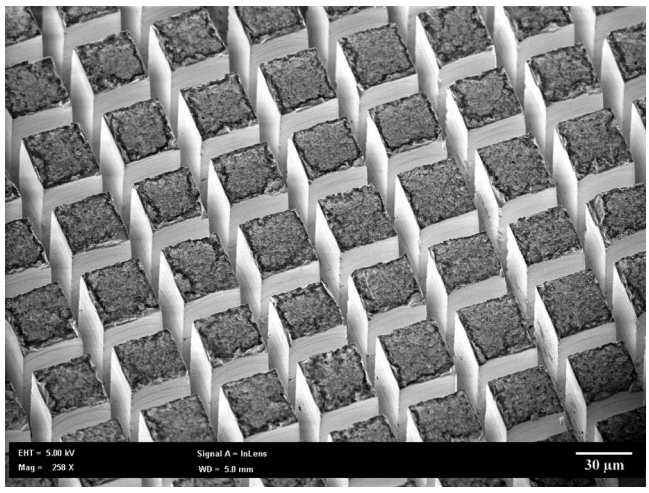

FIG. 4. SEM images of a diced PMN-PT single crystal.

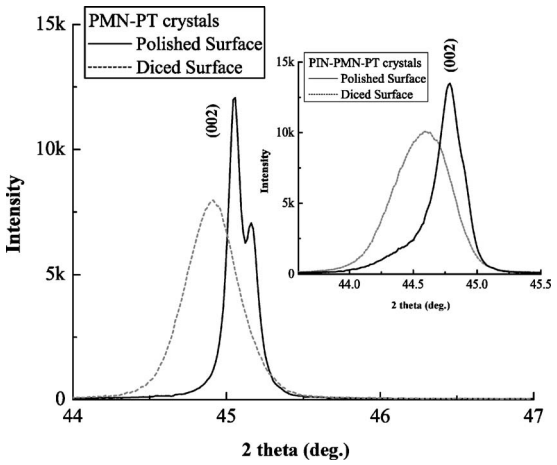

FIG. 5. XRD patterns of as-polished and as-diced surface for PMN-PT and PIN-PMN-PT single crystals.

surface layers.[21,22] Therefore, the degraded properties of PMN-PT 1–3 composites can be strongly attributed to the combination of surface boundary effects and dicing damage, while those of PIN-PMN-PT 1–3 composites are due only to the dicing damage. It should be noted that in composites, the epoxy filler may also play a role in reduced properties, owing to the clamping effect from the epoxy stiffness.[23]

IV. CONCLUSION

In summary, the dielectric and electromechanical properties of relaxor-PT crystals and 1–3 composites were investigated as a function of thickness (500–40 μm) and corresponding ultrasound frequency. The free dielectric permittivity of PMN-PT monolithic crystals was found to be only half of the original value when sample thicknesses decreased to 40 μm (~50 MHz), the underlying mechanism responsible for the degradation is believed to be related to their relatively large domains, being on the order of >10 μm, where the domains were clamped and polarization rotations suppressed, due to the surface boundary effect. As a consequence, the coupling was found to decrease with decreasing sample thickness. Of particular importance is that PIN-PMN-PT crystals exhibited minimal thickness dependent dielectric and electromechanical properties, benefiting from their small domain size ~1 μm.

PIN-PMN-PT 1–3 composites, however, were found to possess lower coupling factors when compared to their monolithic counterparts, being on the order of 84% at 2 MHz, due to the dicing damage and/or low polarizable surfaces, as confirmed by XRD. Of great potential is their yet high couplings, being 80% at 20 MHz, much higher when compared to PMN-PT 1–3 composites, being only 72% at the same frequency, make PIN-PMN-PT crystals promising candidate for high frequency ultrasound. More investigations are underway, including domain size study, mitigation of damage from dicing, alternative composite fabrication methods, such as deep reactive ion etching and porous polymer resin.

ACKNOWLEDGMENTS

This work was supported by the NIH under Grant No. P41-EB21820 and ONR under Grant Nos. N00014-09-1-01456 and N-00014-07-C-0858. The authors thank Dr. Jun Luo and Dr. Wesley Hackenberger from TRS Technologies Inc., for providing the single crystals. Thanks also to Mr. Eugene R. Gerber and Prof Nadine B. Smith from the Department of Bioengineering, Penn State, for help in the fabrication of 1–3 composites.

[1] G. Lockwood, D. Turnball, D. Christopher, and F. Foster, IEEE Eng. Med. Biol. Mag. **15**, 60 (1996).
[2] K. K. Shung and M. Zipparo, IEEE Eng. Med. Biol. Mag. **15**, 20 (1996).
[3] F. S. Foster, C. J. Pavlin, G. R. Lockwood, L. K. Ryan, K. A. Harasiewicz, L. Berube, and A. M. Rauth, IEEE Trans. Ultrason. Ferroelectr. Freq. Control **40**, 608 (1993).
[4] D. Turnbull, B. Starkoski, K. Harasiewicz, J. Semple, L. From, A. Gupta, D. Sauder, and F. Foster, Ultrasound Med. Biol. **21**, 79 (1995).
[5] K. K. Shung, J. M. Cannata, and Q. F. Zhou, J. Electroceram. **19**, 141 (2007).
[6] F. Foster, L. Ryan, and D. Turnbull, IEEE Trans. Ultrason. Ferroelectr. Freq. Control **38**, 446 (1991).
[7] S. Lau, H. Li, K. Wong, Q. Zhou, D. Zhou, Y. Li, H. Luo, K. Shung, and J. Dai, J. Appl. Phys. **105**, 094908 (2009).
[8] P. Sun, Q. Zhou, B. Zhu, D. Wu, C. Hu, J. Cannata, J. Tian, P. Han, G. Wang, and K. Shung, IEEE Trans. Ultrason. Ferroelectr. Freq. Control **56**, 2760 (2009).
[9] S. E. Park and T. R. Shrout, J. Appl. Phys. **82**, 1804 (1997).
[10] S. Zhang, J. Luo, W. Hackenberger, and T. Shrout, J. Appl. Phys. **104**, 064106 (2008).
[11] S. J. Zhang, J. Luo, W. Hackenberger, N. Sherlock, R. J. Meyer, Jr., and T. R. Shrout, J. Appl. Phys. **105**, 104506 (2009).
[12] X. Jiang, K. Snook, W. Hackenberger, and X. Geng, Proc. SPIE **6531**, 65310 F (2007).
[13] X. Jiang, K. Snook, T. Walker, A. Portune, R. Haber, X. Geng, J. Welter, and W. Hackenberger, Proc. SPIE **6934**, 69340D (2008).
[14] www.trstechnologies.com
[15] IEEE Standard on Piezoelectricity (ANSI/IEEE, New York, 1987).
[16] E. C. Subbarao, M. C. McQuarrie, and W. R. Buessem, J. Appl. Phys. **28**, 1194 (1957).
[17] S. Cheng, I. K. Lloyd, and M. Kahn, J. Am. Ceram. Soc. **75**, 2293 (1992).
[18] S. Jyomura, I. Matsuyama, and G. Toda, J. Appl. Phys. **51**, 5838 (1980).
[19] D. Damjanovic, IEEE Trans. Ultrason. Ferroelectr. Freq. Control **56**, 1574 (2009).
[20] H. Fu and R. E. Cohen, Nature (London) **403**, 281 (2000).
[21] L. Lim, F. Kumar, and A. Amin, J. Appl. Phys. **93**, 3671 (2003).
[22] W. Chang, M. Shanthi, K. Rajan, L. Lim, F. Wang, C. Tseng, C. Tu, P. Yang, and H. Moser, J. Appl. Phys. **101**, 124104 (2007).
[23] T. Shiosaki, O. Kobayashi, M. Chisaka, T. Ochi, and H. Kubota, 2009 US Navy Workshop on Acoustic Transduction Materials and Devices, State College, PA, May 12–14, 2009 (unpublished).